Evaluating the Efficiency of Jacked-in Piles as Tsunami Defences

A. DOBRISAN
BA MEng, Department of Engineering, University of Cambridge, Cambridge, UK
Email: ad622@cam.ac.uk
S.K. HAIGH
MA MEng PhD, Department of Engineering, University of Cambridge, Cambridge, UK
Y. ISHIHARA
MA, Construction Solutions Development Department, Giken Ltd., Kochi, Japan

ABSTRACT

The 2011 Tōhoku earthquake and tsunami brought into question the adequacy of the pre-existing shallow foundation seawall design due to the large number of failures recorded. A new type of seawall made of adjoining large, jacked-in, steel pipe piles embedded 10-15m into the ground is currently installed along the Kochi coastline. Seawall design against tsunamis is a unique, true ULS design, which presently is carried out using codes of practice not specifically tailored for this scenario. Through small scale wave flume experiments and lateral loading tests of single piles at full-scale the adequacy of current design methodology as well as the efficiency of the new steel pile seawall design is assessed. It is found that current Japanese codes, although designed for tsunami shelters, provide appropriate predictions of wave force for the case of seawalls needing to withstand overtopping waves. The lateral pile tests highlight the current codes' accuracy in predicting pile stiffness and bending moment profile. Remaining shortcomings, such as no provision in current seawall design for the effects of soil softening during tsunamis, are evinced. Even so, steel pile walls seem an effective seawall solution due to their high embedment and capacity to dissipate wave energy through yielding.

Key words: *Seawall Design, Tsunami, Lateral Resistance, Wave Flume, Steel Piles*

1. Introduction

In the aftermath of the devastating 2011 Tōhoku earthquake and tsunami the large number of seawall failures, exemplified by **Fig. 1** and **Fig. 2** from Kato et al. (2012), evinced a need for a redesign. Instead of the shallow foundation concrete caisson design a new solution currently being installed along the coastline of Kochi prefecture is a seawall made from adjoining large, jacked-in steel pipe piles embedded 10-15m into the ground. An immediate advantage of the new design is its beneficial role even in the case of extremely large waves. This results from the piles' capacity to yield and dissipate wave energy as well as the unlikeliness of piles becoming debris due to the large embedment. These advantages align well with the post-2011 Japanese requirement of seawalls needing to safely withstand overtopping waves (Suppasri et al., 2012).

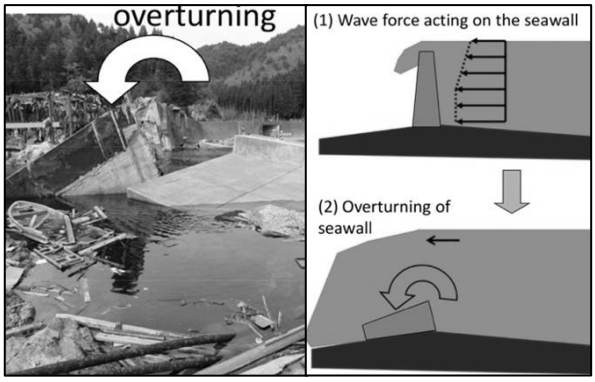

Fig. 1 Seawall overturning (Kato et al., 2012)

Even so seawall design against tsunamis is a unique, true ULS design, which currently is carried out using codes of practice not specifically designed for this scenario.

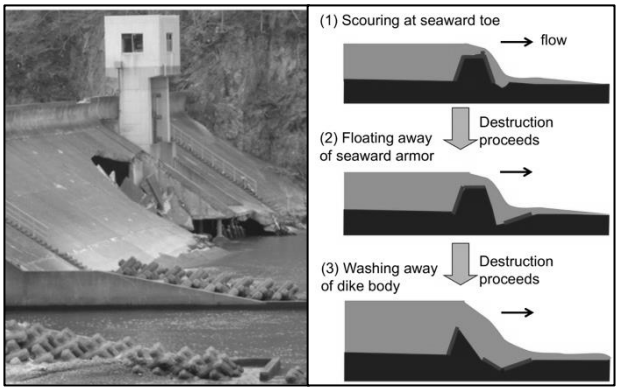

Fig. 2 Scour seawall failure (Kato et al., 2012)

2. Research aims

Through the use of small scale wave flume model experiments and lateral loading tests of piles at full-scale, this paper aims to investigate the adequacy of current design methodology as well as assess the efficiency of the new steel pile seawall design. In designing a seawall against tsunamis the major challenges are estimating the wave force and quantifying the effect of the dynamic nature of the load as well as assessing whether the seawall has the capacity to carry the total loading.

The wave flume experiments are employed to obtain time histories of wave force across multiple scenarios. These forces are compared with predictions from the Japanese code (Okada et al., 2006). Since the code was written with tsunami shelters in mind and the assumption that waves are much smaller than the building size, it does not presently take dynamic amplification into account. The validity of this premise in the case of seawalls can be assessed through the use of the wave force time histories coupled with insight of the pile-soil system stiffness gained from full-scale lateral pile tests.

The full-scale tests on single piles identical to those installed on the Japanese coast also serve to check how well design codes (DNV, 1992) scale to tsunami seawalls. These codes are mostly based on the works of Reese et al. (1974) which analysed data from lateral tests on 0.5-0.6m diameter flexible piles, unlike the much stiffer, 1m diameter piles used in the construction of the new seawalls.

3. Experimental Setup

3.1. Wave flume experiments

The experiments were carried out in the Giken Tsunami Simulator, a 14m long by 2m wide wave flume (**Fig. 3**). Two steel plate model walls, 10cm and 15cm high respectively, were used in these tests. Pressure transducers were fitted along the height of the walls to quantify the wave-wall interaction. Four uniformly spaced transducers

Fig. 3 10cm model wall and wave sensors

were installed on the 15cm high model wall. A denser array of sensors was employed for the 10cm high wall, shown in **Fig. 4**.

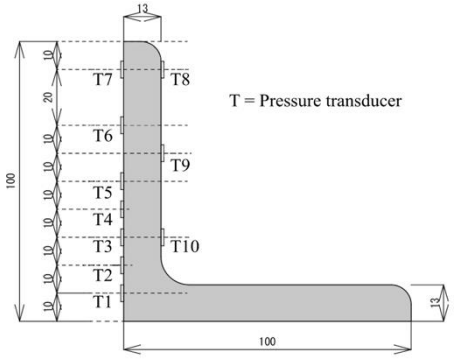

Fig. 4 10cm model wall cross section

A wave height sensor and 2 velocity sensors were fitted in the flume just in front of the test wall. One of the velocity sensor was lowered to the base of the wall, while the other measured water velocities just above the wall as the water passed over. Another height and velocity sensor pair was positioned 4m ahead of the wall to measure the incoming wave characteristics (seen in **Fig. 3**). A total of 47 experiments were carried out in the Tsunami Simulator, with wave heights both greater and smaller than the heights of the walls. A typical initial impact between a wave and model seawall is shown in **Fig. 5**.

Fig. 5 Model tsunami wave hitting wall

3.2. Lateral Pile Tests

Two full-scale lateral pile tests were designed to investigate the performance of a 5m seawall subjected to an overtopping tsunami wave. While a typical seawall is generally comprised of a contiguous row of piles, the behaviour of singular piles is investigated to provide relevant insight. The tests were carried out at the Nidahama test site in Kochi, Japan. A Giken Ltd trial site, next to the Pacific, with sandy soil up to 5m depth and sandy gravel below it, Nidahama closely mimics the ground conditions the pile seawalls were installed in along the Kochi coastline. Three SPTs and two triaxial consolidated drained tests were used to assess ground properties, summarized in **Table 1**. Further information on the test site can be found in Gillow et al. (2018).

Table 1. Derived soil properties at Nidahama test site

Water table depth	γ_t	γ'	R_d	Φ_{crit}	Φ_{peak}
m	kN/m^3	kN/m^3	%	Deg	Deg
7.45	20	12.4	70	32	40

Table 2 highlights the key properties of the two steel tubular piles. The yield stress and the ultimate tensile stress capacities were taken from the manufacturer's specification sheet. However further data from mechanical testing was made available for Pile 2. As can be seen there is a significant factor of safety included in the material properties as quoted by the manufacturer.

The piles were loaded horizontally through a powerful hydraulic jack. To provide reaction a system of 4 steel piles was employed. These had similar properties to the tested piles and their deflection was monitored throughout the test to ensure that the reaction system was sufficiently stiff and was not affecting the experiment. The configuration is shown in **Fig. 6**. The position of the hydraulic jack (2.4m above ground) was chosen as to coincide with the point of application of the equivalent static wave force as described by Okada et al. (2006). An assortment of sensors was used to monitor the pile response during testing: 10 strain gauge pairs were positioned on the pile at 1m intervals below ground, inclinometers were placed at the same sections as the gauges and LVDTs and wire displacement sensors were used to measure accurately the pile displacement at the ground level and at the jack position.

Table 2. Test Piles Key Data

	Dia-meter	*Section Thickness*	*Pile Length*	*Embed-ment*	*Yield Stress*	*Tensile Stress*
	m	mm	m	m	MPa	MPa
Pile 1 (SKK490) specif.	1.0	22	15	10	315	490
Pile 2 (SKK400) specif.	1.0	12	15	10	235	400
Pile 2 (SKK400) measured	1.0	12	15	10	395	504

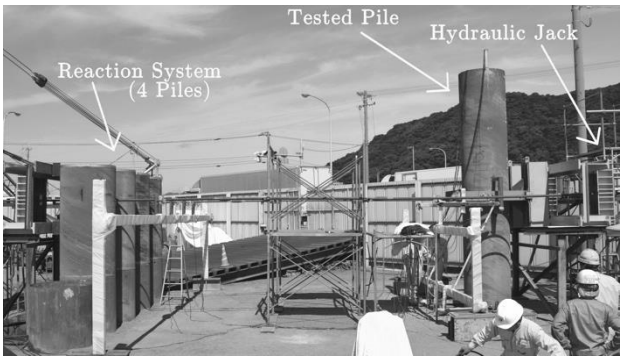

Fig. 6 Lateral pile loading system

The two tested piles were subjected to a small number of unload reload cycles, each cycle having increasing maximum loading. Pile 1 was subjected to 2 cycles, the maximum force overall being 1836kN (corresponding to the observed onset of yielding). Pile 2 was tested up to failure, over 6 cycles and with an input force smaller or equal to 1314kN.

4. Results. Discussions.

4.1. Wave Force Estimation

Fig. 7 shows typical excess water pressures (above baseline hydrostatic) recorded on the model wall during a simulated tsunami wave. To be noticed are the high maxima recorded when the bore hits the wall (highlighted by horizontal bars in **Fig. 7**). These high pressures

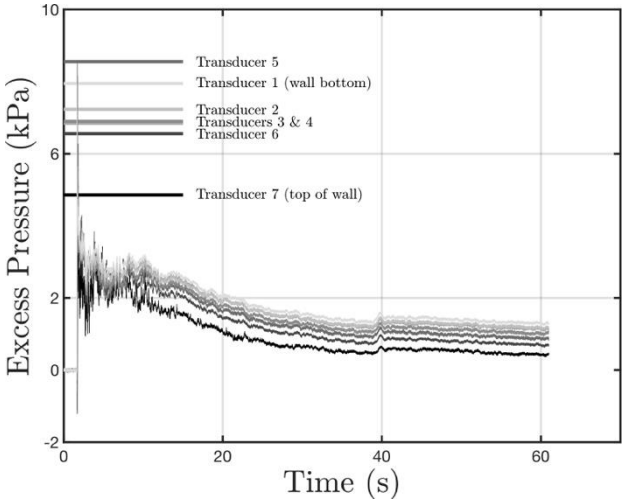

Fig. 7 Excess water pressure vs Time Test 45 (h_{wave} / h_{wall} = 1.45)

presented large variability, with durations between 5-100ms. Furthermore, the peaks did not happen concurrently for all sensors. Lugni et al. (2006) and Kihara et al. (2015) encountered the same phenomena in their wave flume experiments and attributed the irregular behaviour to the adiabatic process of a large amount of air bubbles being mixed in the turbulent bore.

A different way to plot the results is to look at the total force acting on the wall by integrating the pressure values. Since the pressure peaks are asynchronous this reduces their perceived overall effect on the structure. Furthermore, standards of practice generally deal with total wave force acting on structures and as such we can compare our force results to the code values.

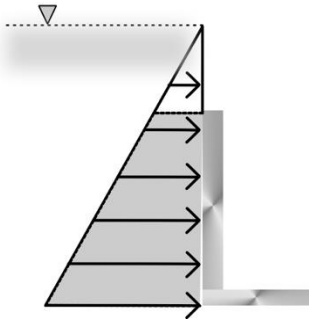

Fig. 8 Trapezium cutout

Okada et al. (2006) consider peak dynamic wave loading as equivalent to a hydrostatic distribution acting on the wall, of height $3xh_{wave}$. Since for most of the wave flume tests $h_{wall} < 3xh_{wave}$ the trapezoidal component of hydrostatic pressure highlighted in **Fig. 8** was integrated to yield maximum predicted surge force.

As exemplified in **Fig. 9** there was large variation in the accuracy of the code surge force prediction across the wave flume tests. To potentially explain the significant scatter, it was observed that the relationship between the measured incoming wave height and velocity in the wave flume did not follow the approximation introduced by Camfield (1980) and further refined by Palermo et al. (2009) of what is characteristic of a tsunami breaking into a turbulent bore:

$$v_{wave} = 2\sqrt{g\, h_{wave}} \qquad (1)$$

where h_{wave} and v_{wave} are the incoming wave properties, far from the model seawall.

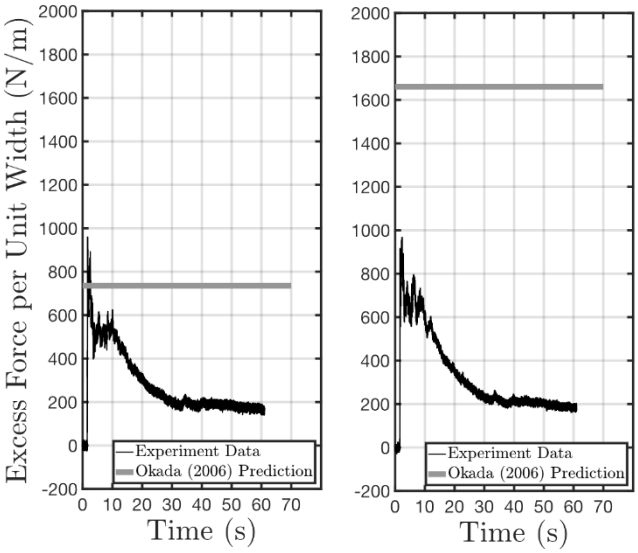

Fig. 9 Measured force against code maximum surge force prediction for two tests on the 15 cm model wall

To further investigate the issue, the hydrostatic and hydrodynamic wave forces were independently derived from the height and velocity sensors at the wall and compared with the total wave force as computed from the pressure transducers. As seen in **Fig. 10** both the hydrostatic and upper hydrodynamic forces predict well by themselves the maximum surge force. Across the 47 wave flume experiments, the hydrostatic force was more consistently a good prediction of maximum surge force than the hydrodynamic force, potentially owing to the fact

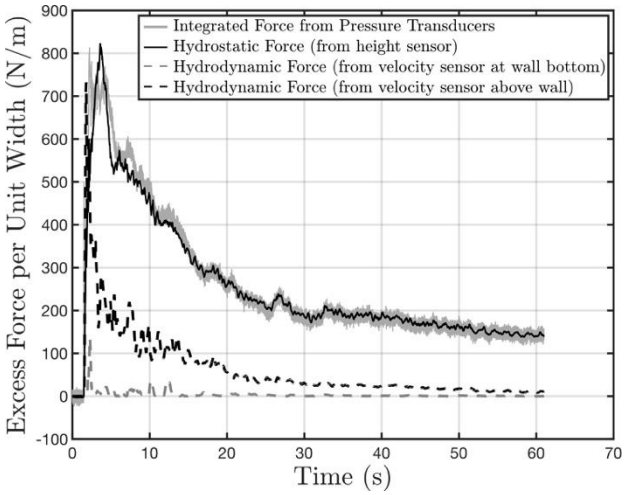

Fig. 10 Wave Force vs Time Test 38 (h_{wave} / h_{wall} = 2.11)

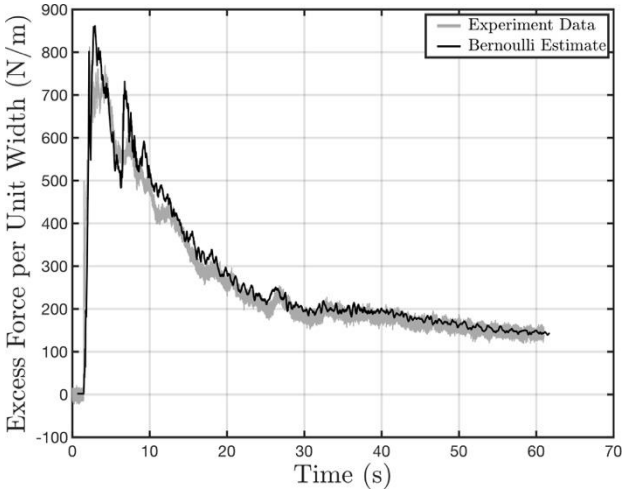

Fig. 11 Bernoulli Estimate vs Time Test 38 (h_{wave} / h_{wall} = 2.11)

that the hydrodynamic result was computed from wave velocity above the wall, assumption which might require adjustment.

The fact that the hydrostatic force at the wall is by itself a good estimate of wave surge force is an encouraging result. A possible interpretation would be that by diverting the wave momentum upwards, the wall experiences the maximum force when the water reaches maximum height and the wave is about to collapse back down on itself.

However it would be beneficial if the water height in front of the model seawall could be inferred from h_{wave} and v_{wave} exclusively as these represent the input parameters, the wave characteristics far from the wall.

Even though the generated wave in the flume is a turbulent bore, if assuming only a small amount of its energy is lost due to turbulent mixing until the wave reaches the wall, Bernoulli's energy conservation along a streamline can be written as:

$$\rho g h + \frac{\rho v^2}{2} = const. \qquad (2)$$

As described above the maximum hydrostatic force on the wall occurs when wave velocity is lowest (corresponding to maximum potential energy). In this assumption, an upper bound for the highest water level in front of the wall can be found by considering the water velocity just in front of the model wall as zero:

$$h_{max} = h_{wave} + \frac{v_{wave}^2}{2g} \qquad (3)$$

This upper bound result, further named the Bernoulli estimate, can be used to compute not just the maximum surge force prediction, but to estimate the wave force profile across the duration of the whole wave flume experiment. As shown in **Fig. 11** the Bernoulli estimate yields encouraging results. The method provides similarly good estimates across all tests, for both model sea walls.

Fig. 12 shows a comparison between the code (Okada et al., 2006) and the Bernoulli estimate in predicting maximum surge force. The comparison includes data from all tests and for both walls by using non-dimensional expressions for force. Even though on average both methods predict the experimental force well, there is significantly less scatter in the Bernoulli results. Thus the Bernoulli estimate significantly improves the

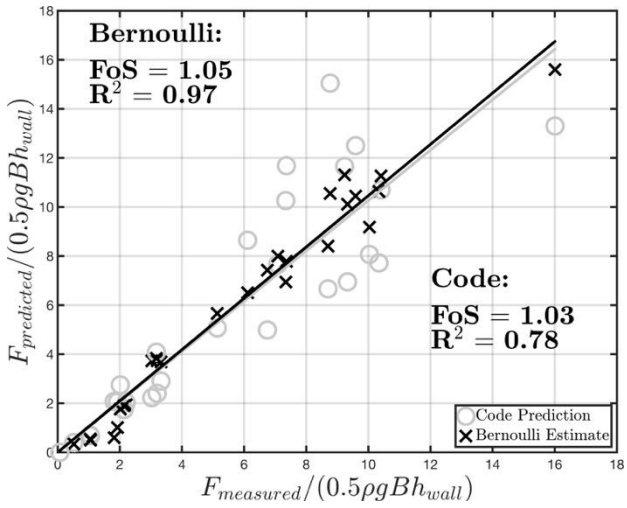

Fig. 12 Non-dimensional Measured vs Predicted Maximum Wave Force

precision of the force estimates over the code (Okada et al., 2006) in the case of the wave flume experiments.

However as stated prior, the waves generated in the wave flume do not have the same link between wave velocity and height as a tsunami. If the Bernoulli estimate is applied for a tsunami, substituting the result of (1) into (3) yields $h_{max} = 3xh_{wave}$. Thus the Bernoulli estimate generally becomes equivalent to the code (Okada et al., 2006) for tsunami waves. This would suggest that although the code was originally designed for the scenario of waves significantly smaller than buildings/seawalls, the methodology still applies for larger tsunami waves, as long as the seawall is able to divert most of the wave momentum upwards. However, if incoming waves are many times greater than the seawall the Bernoulli Estimate would suggest the surge height (and force) will be diminished on account of a significant amount of wave momentum passing over the wall (**Fig. 13**).

Thus, from the wave flume experiments applying current codes will result in a good approximation of actual wave surge force, without however any safety factor built in by default.

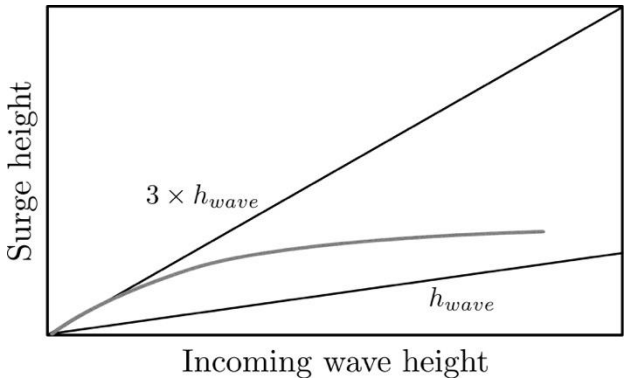

Fig. 13 Tsunami surge height – predicted behaviour

4.2. Lateral resistance of single piles

Fig. 14 shows the force-displacement curve for Pile 1 at the hydraulic jack loading position (2.4m above ground). Pile 1 was tested up to yield. Overlaid on top of the experimental data is the DNV (1992) prediction of the curve given the parameters in **Table 1** and **Table 2**. Even though the standard was designed around smaller and more flexible piles, it applies well for the static loading of the larger diameter piles installed in tsunami seawalls. For the case of initial loading the stiffness is correctly predicted, however the failure load is under-predicted.

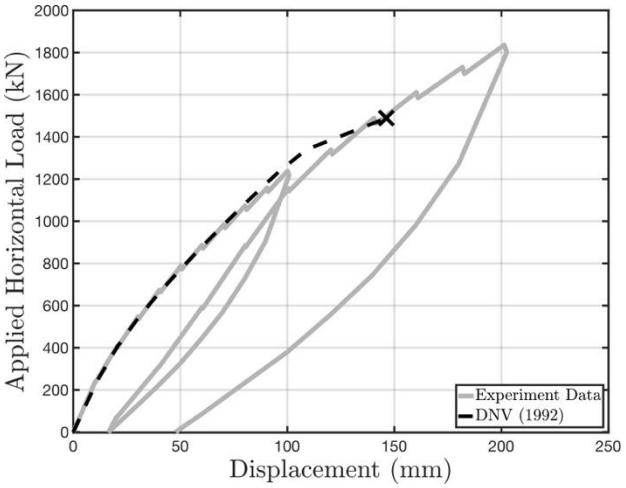

Fig. 14 Pile 1 Horizontal Load vs Displacement

Fig. 15 shows the force-displacement curve for Pile 2, again with the DNV (1992) prediction on top. Stiffness is well predicted in the case of the second pile too, however failure load is again under-predicted if taking into account the manufacturer-specified yield and ultimate tensile stresses. If correcting with the inspection values, as seen in **Fig. 16**, DNV (1992) predicts both stiffness and ultimate strength with good accuracy.

As such an intrinsic safety factor of 2 in the lateral resistance of the piles seems to have been placed in through the steel manufacturer reporting conservative material properties. This cannot be taken for granted as there is variability in the quality of batches even from the same manufacturer. However to note is that the DNV (1992) calculation in itself does not appear to include safety margins.

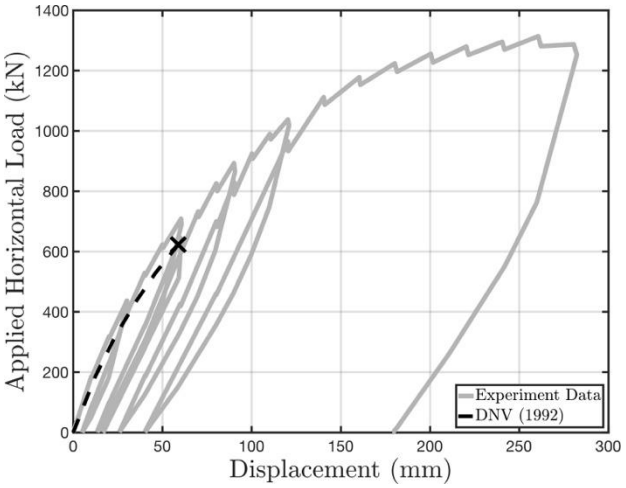

Fig. 15 Pile 2 Horizontal Load vs Displacement (manufacturer specified yield strength)

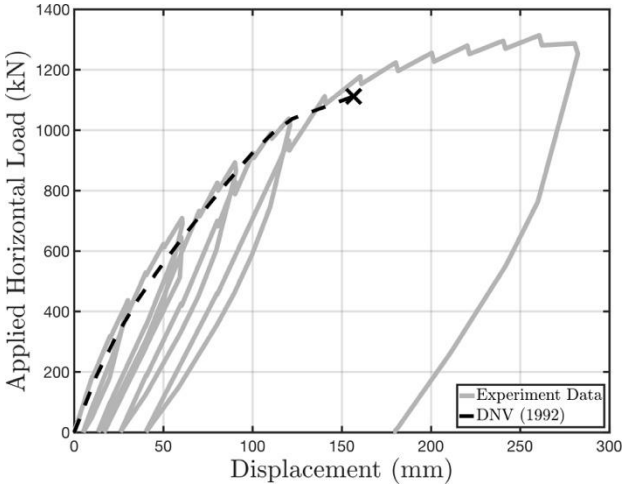

Fig. 16 Pile 2 Horizontal Load vs Displacement (measured yield strength)

From the recorded strain gauge data bending moment can be derived at the sensor locations along the pile for each load increment. Bending moment results provide insight into the way lateral load is carried by the soil-pile system. **Fig.17** shows Pile 1 bending moment data for the instances in which the hydraulic jack applied 673kN and 1238 kN of lateral force respectively. For comparison the DNV (1992) bending moment prediction is also shown in **Fig. 17**. Similar to the case of the load-displacement curves, the code (DNV, 1992) provides an accurate prediction of bending moment, at both low and high loading forces. This holds true for both pile tests.

Moreover from the bending moment profiles in **Fig. 17** it is seen that the region of the pile carrying the highest moment (and thus likely to form plastic hinges first) is the upper half of the embedded length of the pile. The same was found to be true for Pile 2. Hence it would seem that the piles need not be embedded to 10m to withstand the same amount of force. However, a tsunami wave likely induces significant excess pore pressure in the ground as well as high hydraulic gradients between the sides of a seawall. These would lead to reduced effective stress and potentially scouring which would diminish significantly the strength of the soil, especially in the upper layers of the ground, warranting a higher embedment than would result from the static lateral tests.

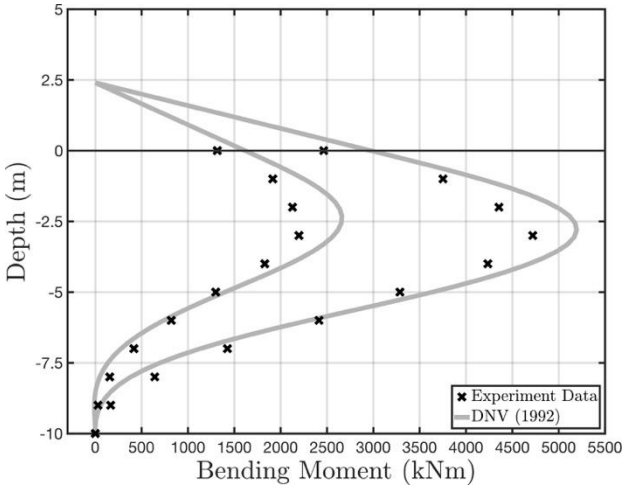

Fig. 17 Bending moment profile with depth at 673 kN and 1238 kN lateral load respectively

4.3. Dynamic amplification

To assess dynamic amplification due to the tsunami loading it is first observed that the wave force in the case of a seawall is driving the wall-soil system, much like the input acceleration from an earthquake drives soil-structure systems into vibrating. Thus, response spectra can be derived in similar fashion for seawalls as for buildings to investigate which structures are most susceptible to damage based on their natural period.

Fig. 18 shows a typical Dynamic Amplification Factor (DAF) spectrum from a wave flume experiment. With amplifications of 70% for certain frequencies the possibility of dynamic amplification for seawalls cannot be trivially neglected. Generally, the flume tests show dynamic amplification occurring mostly for less stiff structures, with longer natural periods, above 0.5s.

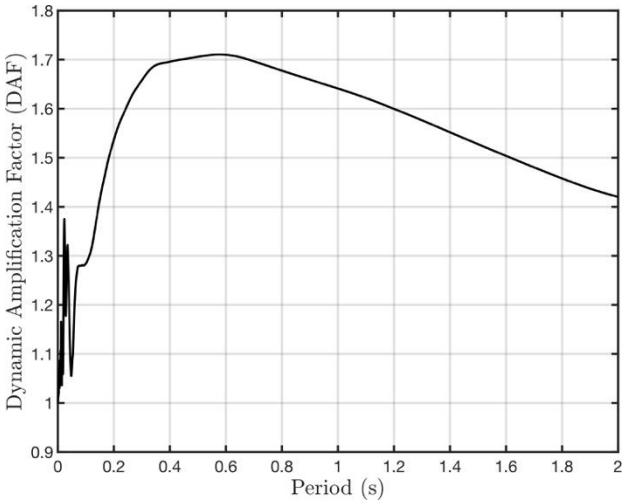

Fig. 18 DAF for a Pile-Soil System with $\zeta = 5\%$ from Wave Loading in Test 34 ($h_{wave} / h_{wall} = 1.95$)

An upper bound for the pile natural frequency can be

computed using the stiffness of the force-displacement curves (**Fig. 14** and **Fig. 16**). It computes to 8Hz, outside the amplification region predicted by the flume tests. Even so, as discussed in section **4.2**, stiffness degradation due to soil softening can reduce the natural frequency considerably and hence make dynamic amplification relevant and potentially dangerous.

5. Concluding remarks

Through wave flume and lateral pile tests it has been shown current codes of practice generally scale up well to the case of large tsunami seawalls.

The wave flume results show current codes in Japan (Okada et al., 2006) designed for tsunami shelters provide appropriate predictions of wave force for the case of a seawall built to withstand overtopping waves.

Full-scale lateral pile tests were carried out to check whether codes derived from data on smaller, more flexible piles, are appropriate in the tsunami seawall scenario. The results show current codes (DNV, 1992) predict stiffness, displacement as well as bending moment profile with high accuracy.

However, there are still shortcomings due to the codes not being specifically developed for the tsunami use case. The effect of soil softening during the tsunami, currently not explicitly taken into account in design, may be significant. It leads to reduced seawall resistance and potentially to an increase in apparent wave load through dynamic amplification. As a consequence, more research is required to tackle the problem of seawall design against high tsunami waves specifically.

That being said, despite remaining unknowns, steel pile walls seem to be an effective seawall solution. This is due both to the high embedment which mitigates some of the problems associated with soil softening, but also to their capacity to be useful beyond yield, continuing to absorb wave energy by means of plastic deformation.

6. Acknowledgements

The authors would like to thank Giken Seisakusho Ltd. for funding this work through the Giken-Cambridge collaboration. Acknowledgements must be paid to President Kitamura for the continued success of this collaboration.

References

Camfield, F.E. 1980. Tsunami Engineering. Special Report No. 6. US Army Eng. Waterw. Exp. Stn. Coast. Eng. Res. Cent. Vicksbg. Miss., pp. 222.

DNV. 1992. Foundations (No. 30.4). Det Norske Veritas.

Gillow, M., Haigh, S.K., Ishihara, Y. 2018. Water Jetting for Sheet Piling, in: The First International Conference on Press-in Engineering. Kochi, Japan.

Kato, F., Suwa, Y., Watanabe, K., Hatogai, S. 2012. Mechanisms of coastal dike failure induced by the Great East Japan Earthquake Tsunami. Coastal Engineering Proceedings, 1 (33).

Kihara, N., Niida, Y., Takabatake, D., Kaida, H., Shibayama, A., Miyagawa, Y. 2015. Large-scale experiments on tsunami-induced pressure on a vertical tide wall. Coastal Engineering, 99, pp. 46–63.

Lugni, C., Brocchini, M., Faltinsen, O.M. 2006. Wave impact loads: The role of the flip-through. Phys. Fluids, 18 (12), pp. 122101.

Okada, T., Sugano, T., Ishikawa, T., Takai, S., Tateno, T., 2006. Tsunami loads and structural design of tsunami refuge buildings. The Building Centre of Japan.

Palermo, D., Nistor, I., Nouri, Y., Cornett, A. 2009. Tsunami loading of near-shoreline structures: a primer. Canadian Journal of Civil Engineering. 36 (11), pp. 1804–1815.

Reese, L.C., Cox, W.R., Koop, F.D. 1974. Analysis of laterally loaded piles in sand. Offshore Technological Conference, Houston, Texas, pp. 473-483.

Suppasri, A., Koshimura, S., Imai, K., Mas, E., Gokon, H., Muhari, A., Imamura, F. 2012. Damage Characteristic and Field Survey of the 2011 Great East Japan Tsunami in Miyagi Prefecture. Coastal Engineering Journal. 54 (1), 1250005.